

Article

Transcriptome of *Arabidopsis thaliana* Plants Exposed to Human Parasites *Cryptosporidium parvum* and *Giardia lamblia*

Yaroslav Ilynyskyy¹, Andrey Golubov¹, Boseon Byeon² and Igor Kovalchuk^{1,*} 

¹ Department of Biological Sciences, University of Lethbridge, University Drive 4401, Lethbridge, AB T1K 3M4, Canada; slava.ilyntskyy@uleth.ca (Y.I.); agolubov@gmail.com (A.G.)

² Biomedical and Health Informatics, Computer Science Department, State University of New York, 2 S Clinton St, Syracuse, NY 13202, USA; boseon.byeon@oswego.edu

* Correspondence: igor.kovalchuk@uleth.ca

Abstract: Pathogen infection in animals and plants is recognized in a relatively similar manner by the interaction of pattern recognition receptors on the host cell surface with pathogen-associated molecular patterns on the pathogen surface. Previous work demonstrates that animal pathogenic bacteria can be recognized by plant receptors and alter transcriptome. In this work, we have hypothesized that exposure to human parasites, *Cryptosporidium parvum* and *Giardia lamblia*, would also trigger pathogen response in plants, leading to changes in transcriptome. Detached *Arabidopsis* leaves were exposed for one hour to heat-inactivated *Cryptosporidia* or *Giardia*. The transcriptome profile showed large changes in gene expression with significant overlap between two parasites, including upregulated GO terms “cellular response to chitin”, “response to wounding”, “response to oomycetes”, “defense response to fungus”, “incompatible interaction”, and “activation of innate immune response”, and downregulated GO terms “positive regulation of development”, “cell surface”, “regulation of organ growth”, “wax biosynthetic process”, “leaf and shoot morphogenesis”. Uniquely downregulated GO terms in response to *Cryptosporidia* were GO terms related to chromatin remodelling, something that was not reported before. To conclude, it appears that while *Cryptosporidia* or *Giardia* are not pathogens of *Arabidopsis*, this plant possesses various mechanisms of recognition of pathogenic components of parasites.

Keywords: *Cryptosporidium parvum*; *Giardia lamblia*; *Arabidopsis thaliana*; transcriptome profiling



Academic Editor: Adriano Sofò

Received: 17 December 2024

Revised: 6 January 2025

Accepted: 13 January 2025

Published: 18 January 2025

Citation: Ilynyskyy, Y.; Golubov, A.; Byeon, B.; Kovalchuk, I. Transcriptome of *Arabidopsis thaliana* Plants Exposed to Human Parasites *Cryptosporidium parvum* and *Giardia lamblia*. *Int. J. Plant Biol.* **2025**, *16*, 13. <https://doi.org/10.3390/ijpb16010013>

Copyright: © 2025 by the authors. Licensee MDPI, Basel, Switzerland. This article is an open access article distributed under the terms and conditions of the Creative Commons Attribution (CC BY) license (<https://creativecommons.org/licenses/by/4.0/>).

1. Introduction

Humans can be infected with parasitic organisms through consumption of contaminated food and/or water [1]. Moreover, consumption of fresh plants can also lead to infection with pathogens [2]. These pathogens do not necessarily cause the disease in plants, and typically have lower virulence while outside their host (human or another animal).

Bacterial and parasitic infection is initially recognized by interaction between pathogen-associated molecular patterns (PAMPs) on the pathogen surface and receptors known as pattern recognition receptors (PRR) on the host surface [3]. While Toll-like receptors (TLR) are the receptors that belong to the PRR group [4], PAMPs represent a versatile group of molecules, typically proteins or lipopolysaccharides (LPS) [5]. Recognition of pathogenic components typically leads to the activation of defence mechanisms, often resulting in resistance to recognized pathogens [6]. For example, in animals, LPS and glycoproteins (such as from *Giardia lamblia* (*G. lamblia*)) are recognized by TLR2 and TLR4 receptors [7].

PAMP recognition activates a cascade of defensive responses, including production of various pro-inflammatory cytokines including IL-6, IL-12, TNF- α , as well as various other inflammatory mediators [8] (Espinosa-Riquer et al., 2020).

Parasites are recognized in animals and plants in a similar manner through the activation of PRRs by PAMPs. PRRs in the form of nucleotide-binding and oligomerization domain (NOD)-like receptors (NLRs) are similar in structure and function between plants and animals. As a result, it appears that several pathogens can infect both animal, and plant species [9,10]. As plants do not have adaptive immunity, they protect themselves against pathogens through a two-tiered system, PAMP and microbial-associated molecular patterns (MAMPs) or damage-associated molecular patterns (DAMPs) that are recognized by PRR. This leads to pattern-triggered immunity (PTI) to be initiated [11]. For example, surface receptor-like protein CUSCUTA RECEPTOR 1 (CuRe1) was shown to be essential for the perception of parasite-associated molecular pattern of *Cuscuta reflexa* parasite in tomato [12]. When PTI fails or suppressed, a second line of defense, Effector-Triggered Immunity (ETI), is initiated; ETI is initiated upon recognition of pathogenic effectors by NB-LRR proteins (resistance genes) and results in hypersensitive response and isolation of a pathogen at a place of infection [13].

PTI similarity between animals and plants is shown by the induction of immune response in *Arabidopsis thaliana* (*A. thaliana*) by *Salmonella enterica* flagellin; this response was shown to be dependent on active FLS2 protein [10]. Also, we previously demonstrated that the response of *A. thaliana* to pathogenic *E. coli* O157:H7 is partially FLS2 dependent, since the transcriptomic response of the *fls2* mutant was substantially different from the wild-type *A. thaliana* plants [14]. Similar FLS2 dependence in response to another human intestinal pathogen, *Campylobacter jejuni* (*C. jejuni*), was shown in *A. thaliana* [15]. We found that the response of *fls2* mutant plants to *C. jejuni* was more robust on the level of transcription; we also found that the response of the wild type *A. thaliana* to *E. coli* O157:H7 and *C. jejuni* was more similar than the response of the *fls2* mutant plants, suggesting that there are FLS-independent mechanisms of recognition of these two bacteria, and they differ [15].

In this work, we tested two human parasites, *Cryptosporidium parvum* (*C. parvum*) and *G. lamblia*, for their ability to affect the transcriptome of *A. thaliana*. Zoonotic enteric protozoa parasites like *C. parvum* and *G. lamblia* are recognized by the host immune system through their glycoproteins [16]. The exact receptors involved in the recognition of *C. parvum* are unknown, but likely this recognition is dependent on NOD-like receptors (NLR), such as the NLR family pyrin domain containing 6 (NLRP6), with glycoproteins gp30, gp40/15, and gp900 playing an essential role [6]. Activation of NLRP6 leads to inflammasome-dependent release of the pro-inflammatory cytokine IL-18 playing an essential role in the pathogenesis of parasitic infection [17].

It is not clear whether human parasites are able to colonize plants and whether they are able to induce the production of DAMPs. Therefore, we exposed *A. thaliana* (Col-0) plants to *C. parvum* and *G. lamblia*. We found a large number of dysregulated genes, with most of them being common between the two pathogens. GO term analysis revealed upregulation of pathogen response genes and downregulation of growth, development, and morphogenesis. This suggests that human pathogens can also be recognized by plant machinery.

2. Materials and Methods

2.1. Experimental Set Up

Wild type *Arabidopsis thaliana* plants (Columbia-0) were used in this experiment. Seeds were placed for 48 h at 4 °C on potting soil and then moved to germinate and grow in 10 × 10 cm pots on soil at 16/8 day/night conditions at 22 °C.

The *Giardia intestinalis* (Lambl) Alexeieff (*G. intestinalis*) is the clone of WB strain ATCC 50803. The *Cryptosporidium parvum* (*C. parvum*) is the strain AZ1, a *C. parvum* Type II originally isolated from an AIDS patient. Both strains were prepared by Hyperion Research Ltd. (Medicine Hat, AB, Canada). *Giardia* was prepared at the concentration of 2×10^6 cysts per mL, while *Cryptosporidium* at 5×10^6 oocytes per mL of 1x PBS at pH 7.2. Both were killed by irradiation with 400 mJ/cm² UVC at 254 nm.

Plants were used for buffer treatment or treatment with a pathogen. Each treatment was performed twice, representing biological replicates. For treatments, fully expanded leaves of 3-week-old plants were cut and placed into 14 mL falcon tubes filled with Murashige and Skoog (MS) medium (six to eight leaves per tube; two plants per each experimental group). Before the treatment, MS medium was discarded, and tubes were filled with 12 mL suspension of *Giardia* or *Cryptosporidium* in PBS (“pathogen” treatment group). A control group was prepared by filling the tube in with PBS (“buffer” treatment group). All work was performed in an operating Class II A2 biological safety cabinet at room temperature within a containment level 2 facility at the University of Lethbridge. Leaf tissues were submerged in the pathogen suspension or PBS for 2 h, washed three times with PBS, and then flash-frozen in liquid nitrogen.

2.2. Total RNA Purification

For the RNA extraction, frozen leaves were ground in liquid nitrogen and the total RNA was purified using TRIzol[®] Reagent (Invitrogen, Thermo Fisher Scientific, High River, AB, Canada) according to instructions provided by the manufacturer. The quality and the concentration of each RNA sample were analyzed using the NanoDrop 2000C spectrophotometer (Thermo Fisher Scientific, High River, AB, Canada). RNA integrity was analyzed using Bioanalyzer RNA 6000 Nano assay (Agilent Technologies, Inc., Santa Clara, CA, USA).

2.3. mRNA Deep Sequencing, Demultiplexing and Sequence Assembly

For mRNA sequencing, the libraries were prepared from total RNA from three experimental groups, non-treated, buffer-treated and bacteria-treated plants, each in two biological replicates. Libraries were prepared according to the instructions for TruSeq RNA sample Prep v2 LS protocol (Illumina, San Diego, CA, USA). In brief, mRNA was extracted from the total RNA using poly-T oligo-attached magnetic beads. After cDNA synthesis, fragmentation and blunting the ends, indexing adapters were ligated to the ends, and the DNA fragments with adaptors on both ends were amplified using limited-cycle PCR method (15 cycles). The libraries were then quantified using the qPCR and analyzed using Agilent DNA 1000 chip (2100 Expert Software, Agilent Technologies, Santa Clara, CA, USA). The libraries were then normalized, pooled, and used for cluster generation using a cBot (Illumina). After that, the single-end 72 cycles sequencing was performed on the Illumina GAIIx.

Base calling and demultiplexing of reads were performed using the CASAVA v1.6 and Novobarcode software (Novoalign V4.03.01, accessed on 14 February 2017). FastQC v 0.10.1 was used for the preliminary quality check. Reads were mapped *Arabidopsis* genome using TopHat v 2.0.4 beta [18]. Transcripts were assembled [19] and the assemblies were merged using the cuffmerge tool (Cufflinks v 2.0.2) with *Arabidopsis* genome

as the reference. Cuffdiff tool (Cufflinks v 2.0.2) was used to assess relative transcript abundance [20].

2.4. Obtaining the List of Differentially Expressed Genes

2.4.1. Quality Control, Sample Clustering and Detection of Differentially Expressed Genes with DESeq2

Count data was loaded into R, normalization and variance stabilizing transformation [21] were applied using DESeq2 package. Normalized and variance stabilized data was used in subsequent quality control and sample clustering analysis. Euclidean sample distances were calculated in R, samples clustering was performed using `hclust()` function in R. Sample to sample distances were visualized as a heatmap.

Principal components plot of the samples was obtained using `PCAplot()` function available in DESeq2 package.

Gene variances were established for all 3 conditions simultaneously using likelihood ratio test (LRT) as described in DESeq2 manual. Separate comparisons of interest: PBS vs. Crisp and PBS vs. Gyr were extracted to obtain differentially expressed genes.

Genes differentially expressed between *Control* (PBS-treated) and *Treated* (either *Giardia* or *Cryptosporidia*) conditions were detected using Wald test on normalized count data as described in DESeq2 manual. Multiple comparisons correction procedure was done with Benjamini-Hochberg correction implemented in R. Genes with adjusted *p*-values (`padj` column) less than 0.05 were considered differentially expressed.

Relationship between mean gene expression levels and log₂ fold change were visualized as MA-plot, red dots on the MA plot show differentially expressed genes with FDR adjusted *p*-value < 0.05.

2.4.2. Detection of Differentially Expressed Genes and Transcripts with NOISeq

Raw count data obtained as described in 2.5.1 was loaded into R and used to detect differentially expressed genes between control group (PBS) and infection groups (Crisp and Gyr) in two separate pairwise comparisons. Statistical tests were performed as described in NOISeq manual. The trimmed mean of M-values (TMM) normalization procedure [22] was applied to normalize raw counts data. The type of replicate used in NOISeq statistical test was “technical”. The rest of the parameters were kept as defaults. Genes with probability value (“`prob`”) more than 0.95 were considered to be differentially expressed. The results of the NOISeq comparison can be found in NOISeq/directory located in `gene_level_analysis` folder.

Relationship between log₂ fold change values (M) and differences between condition (D) were visualized as scatter plots with differentially expressed genes (`prob` > 0.95) shown as red dots.

2.5. Gene Ontology and Pathway Analysis

List of differentially expressed genes detected with NOISeq was used to find significantly overrepresented GO categories and KEGG pathways. Over-represented GO categories and pathways were detected using GOstats Bioconductor package [23]. Alternatively, topGO package (<http://rpackages.ianhowson.com/bioc/topGO/> (accessed on 23 March 2018)) was used to explore significantly enriched GO categories only. The results of topGO and GOstats analysis can be found in topGO/and GOstats analysis folders located in `gene_level_analysis/NOISeq/directory`.

The analysis was done on all of the differentially expressed genes and on up- and downregulated genes separately. Out of 3 components of GO classification only biological process (BP) category was analyzed. Biochemical pathways annotation were obtained from org.At.tair.db Bioconductor package. *p*-value cutoff was set at 0.01 to consider a GO

category significantly over-represented, for KEGG pathways this cutoff was set at p -value of 0.1. In topGO analysis GO categories with elimKS (p -value in elimination test) <0.01 were considered significantly enriched. Top 5 most over-represented GO categories were visualized as an acyclic graph where top 5 nodes are shown as squares and the nodes with lower p -values received more intense shade of red color.

Pathview [24] Bioconductor package was used to display pathway diagrams for select significantly over-represented KEGG pathways.

2.6. Selecting Candidate Genes

Few candidate genes were selected based on very low (0 or almost zero) base line expression in control group that increases many-fold (hundreds or thousands of times) in treated. The selection was done as follows: the files containing the results of statistical testing performed using either DESeq or NOISeq were sorted by log₂ fold change and p -value. Out of top 10 genes obtained after sorting we selected those that were in top 10 detected by both methods: NOISeq and DESeq2.

2.7. Real Time RT-PCR for Confirmation of Gene Expression

Total RNA was treated with DNase I (ThermoFisher Scientific, Lenexa, KS, USA) according to manufacturer's instructions. Briefly, RNA was treated in a total volume of 50 μ L containing 5 μ L of the 10x DNase I buffer (supplemented with MnCl₂), 25 μ L of total RNA, 2 μ L of DNase I (1 U/ μ L), and 18 μ L of UltraPure Distilled Water (Invitrogen, Carlsbad, CA, USA). Reaction was carried out at 37 °C for 30 min. Reaction mixture was purified using phenol: chlorophorm: isoamyl alcohol (25:24:1) mix and precipitated using 1/10 vol of the 3 M sodium acetate (pH 5.2) solution and 2.5 volumes of the 96% ethanol. Precipitate was washed twice in 1 mL of 75% ethanol and once in 1 mL of 96% ethanol, air-dried and dissolved in 20 μ L of UltraPure Distilled Water (Invitrogen, Carlsbad, CA, USA). 500 ng of total RNA from every tissue in 2 biological replicates was treated with DNase I, purified, converted into cDNA and quantified with qPCR. The quantitative real-time PCR was performed using SsoFast EvaGreen Supermix (Bio-Rad, Hercules, CA, USA). Primers for the real-time quantitative PCR were designed using the Beacon Designer7 program (Table 1). The optimization of the annealing temperature, melt-curve analysis, and the analysis of amplicons via gel electrophoresis was done for each set of primers. Tubulin was used as a control. To evaluate the PCR efficiency, the standard curve was established using a series of cDNA dilutions. qPCR reaction was done with the following conditions: one cycle at 95 °C, 10', followed by 42 cycles of 95 °C, 30'' + T, 30'' + 72 °C, 30'', followed by single cycle of 72 °C, 2'.

2.8. Software Versions Used

The following software versions were used: FastQC version 0.11.4; TopHat v2.0.10; bowtie v. 1.1.2; subread-1.5.0; R version 3.2.4 (10 March 2016); Bioconductor version 3.2; DESeq2_1.10.1; NOISeq_2.14.1; biomaRt_2.26.1; pathview_1.10.1; Gostats_2.36.0; org.At.tair.db_3.2.3.

2.9. Statistical Treatment of the Data

Statistical treatment for the sequencing data is described above. For the real time RT-PCR, the average and standard errors of the mean were calculated. Statistical comparison on treatments was confirmed by performing pairwise Students t -tests using the MS Excel software, version 2018 (Microsoft, Redmond, WA, USA).

Table 1. RT-PCR confirmation of selected genes with log2 > 8.

Gene_id	log2	RT-PCR, Fold	Symbol: Description	Primers
Common				
AT5G12030	11.14	9.83	AT-HSP17.6A: Encodes a cytosolic small heat shock protein with chaperone activity that is induced by heat and osmotic stress.	Forward: 5' AGTTTGGGAAG GTTTCCAATA 3' Reverse: 5' GTCCCTCTGT CTTTTGCCAC 3'
AT1G07160	9.93	5.78	NA: Protein phosphatase 2C family protein	Forward: 5' TCCGCCGCG TCTCCCACATC 3' Reverse: 5' ACAAGTTCTT AGCCGCAAAC 3'
AT1G22810	9.25	12.51	NA: DREB subfamily A-5 of ERF/AP2 transcription factor family	Forward: 5' GGATTACAGA GAATCCACC 3' Reverse: 5' GCGTAATGG CCATGCCGGC 3'
AT5G64750	8.80	29.43	ABR1: A member of the ERF (ethylene response factor) subfamily B-4 of ERF/AP2 transcription factor family. Expressed in response to ABA, osmotic stress, sugar stress and drought.	Forward: 5' CGCAGCAGC CGCCTCCATC 3' Reverse: 5' ATACTCGTAT GTTGGGCC 3'
Unique Giardia				
AT1G53540	10.83	27.24	NA: HSP20-like chaperones superfamily protein	Forward: 5' ATTCCAAGC ATCTTCGGAGG 3' Reverse: 5' TCTCTTCATT CTCATGCTC 3'
AT4G25200	9.33	14.69	AtHSP23.6-Mito: nuclear gene encoding mitochondrial protein	Forward: 5' CTCTCGCTCT TAAGAGACTC 3' Reverse: 5' ACAGAGGATT CTCCATGAAC 3'
AT5G12020	8.56	7.32	HSP17.6II: 17.6 kDa class II heat shock protein	Forward: 5' AATAATCTCA ATCCTCGAAG 3' Reverse: 5' ACTGAAACTT CCTCATGAAC 3'
Unique Cryptosporidia				
AT1G51820	9.58	22.90	NA: Leucine-rich repeat protein kinase family protein	Forward: 5' TCAGATGCCG ATTTAGTAGC 3' Reverse: 5' TGAATTGCT AATATACCCTC 3'
AT5G01380	9.20	32.11	NA: Homeodomain-like superfamily protein	Forward: 5' CCAACATCAC CACCACCACC 3' Reverse: 5' GGGAACTGC TGCCTAATAGC 3'
AT5G52400	8.58	13.85	CYP715A1: member of CYP715A	Forward: 5' AAGAAGCTTA GAGGAAACGG 3' Reverse: 5' TGTCGTGT CCAATCATCTCC 3'
AT5G55090	8.52	9.66	MAPKKK15: member of MEKK subfamily	Forward: 5' GGACCAATCA TAGGTCGAGG 3' Reverse: 5' CTTCGCAAT CTCTCCTCCG 3'
AT1G71520	8.42	15.48	NA: encodes a member of the DREB subfamily A-5 of ERF/AP2 transcription factor family	Forward: 5' ATGTCCATAT CTCATAACCC 3' Reverse: 5' CTACGGCAG CGCCTTCTGCGGTGG 3'

3. Results and Discussion

3.1. Clustering and DEGs Analysis Using DESeq and NOISeq

The number of sequencing reads ranged from 4.8 to 9.9 mln, with over 96% of them mapping to the Arabidopsis genome (Supplementary Table S1). Clustering analysis showed complete separation of control samples and parasite-treated samples (Figure 1).

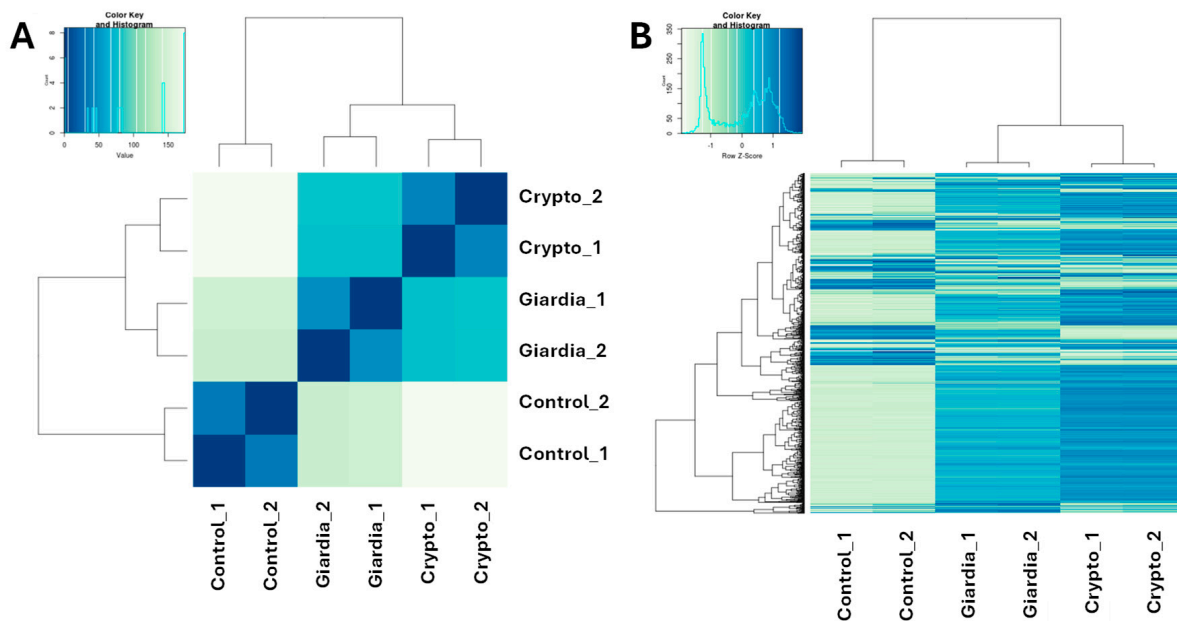


Figure 1. (A). Heatmap showing Euclidean distances between samples calculated with variance transformed data. Samples were clustered with `hclust()` function with default settings. (B). Heatmap of top 1,000 DEGs obtained using DESeq.

To analyze the differentially expressed genes (DEGs), we used two different approaches, DESeq and NOISeq.

For DESeq, we set the significance at $p < 0.05$ and fold difference at $-1 > \log_2 > 1$. Exposure to Giardia resulted in 2469 upregulated and 1767 downregulated genes (see the entire list in Supplementary File S1). Exposure to Cryptosporidium upregulated 3052 and downregulated 2609 genes (see the entire list in Supplementary File S2). Figure 1B shows the heat map and dendrogram of the top 1000 DEGs, demonstrating complete separation of samples.

For NOISeq, the significance was based on the probability test (see Methods) and the probability value of >0.95 , and the fold difference at $-1 > \log_2 > 1$. Exposure to Giardia resulted in 1675 upregulated and 714 downregulated genes (see the entire list in Supplementary File S3). Exposure to Cryptosporidia resulted in 2207 genes upregulated and 1263 genes downregulated (see the entire list in Supplementary File S4). Heat map with cluster analysis shows the overall lower number of DEGs in the NOISeq test, likely due to more stringent conditions applied by this type of analysis. DEGs were visualized using Volcano plots (Figure 2).

We then analyzed the overlap between DESeq and NOISeq analyses for Giardia and Cryptosporidium. We found that all DEGs from NOISeq are accounted for in DESeq (Figure 3A,B). It appeared that the number of unique DEGs found by DESeq was much higher for the downregulated group than for the upregulated group, regardless of the pathogen (Figure 3A; Supplementary File S5). We then analyzed the overlap between Cryptosporidia and Giardia and found that most of DEGs overlapped, with Cryptosporidia having significantly higher number of unique DEGs as compared to Giardia group (Figure 3C,D). We could not find any comparable data in plants, but in human, there was a significantly larger increase in the number of DEGs in response to Cryptosporidia [25] (Sun et al., 2022) as compared to Giardia [26,27] (Tako et al., 2013; Yang et al., 2024), although, it should be noted that these analyses were done using different cells and exposure times, and thus may not be directly comparable.

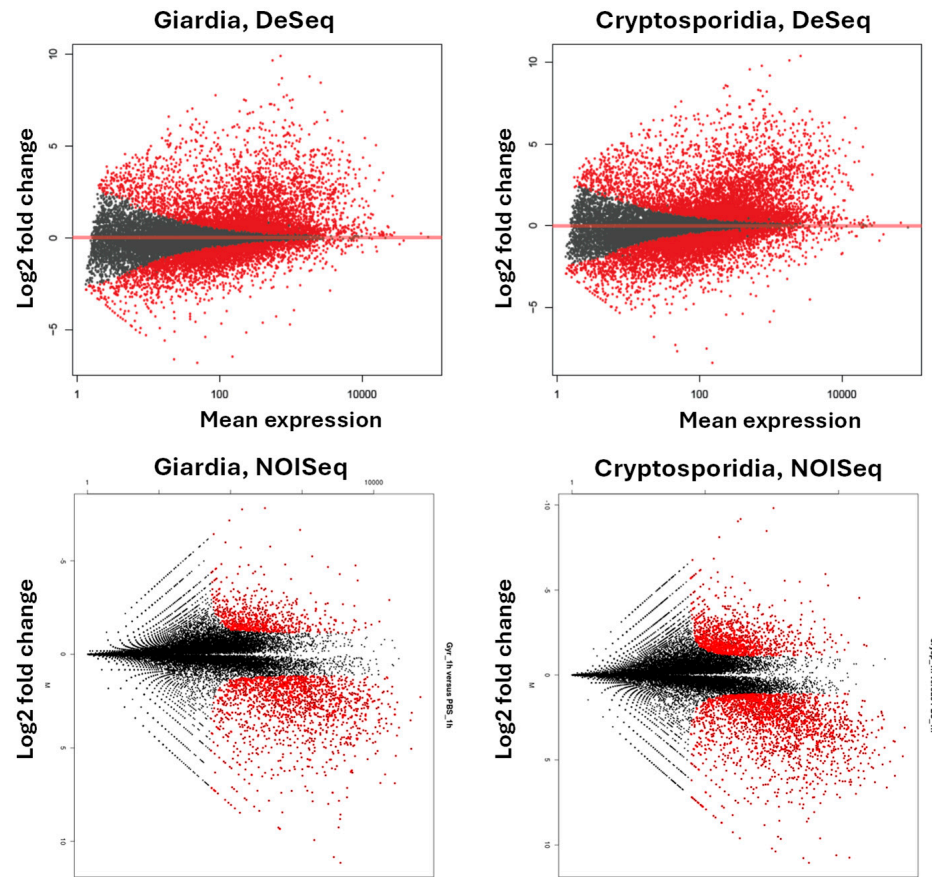


Figure 2. Volcano plot visualization of DEGs using DESeq and NOISeq methods. Y axis shows log₂ fold difference between treatment and control. X axis shows the mean expression level of genes. Red dots show significantly differentially expressed genes.

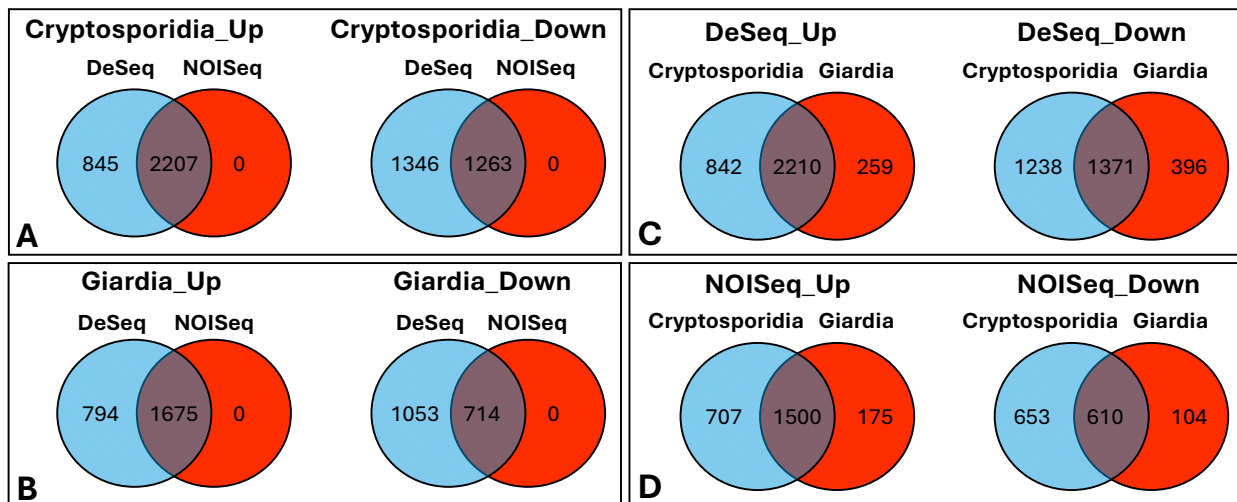


Figure 3. Overlap between DEGs. (A). Overlap between DEGs found by DESeq and NOISeq methods for Cryptosporidia. (B). Overlap between DEGs found by DESeq and NOISeq methods for Giardia. (C). Overlap between DEGs in Cryptosporidia and Giardia found using DESeq method. (D). Overlap between DEGs in Cryptosporidia and Giardia found using NOISeq method.

3.2. GO Term Analysis of DEGs

To identify the pathways uniquely and commonly altered by pathogens, we performed GO term analysis of the DEGs identified only by DESeq approach, since it

included all genes identified by NOISeq as well (Figure 3C). A complete list of all significantly different GO terms is presented in Supplementary File S5 and visualized in Supplementary Figures S1–S7. Table 2 shows selected representative examples of GO terms.

Table 2. GO terms commonly and uniquely differently regulated in response to *Giardia* and *Cryptosporidia*.

Term/Regulation	Fold Enrichment	Term/Regulation	Fold Enrichment
COMMON UPREGULATED		<i>Giardia</i> UPREGULATED	
cellular response to chitin	10.90	response to heat	8.38
oligopeptide binding	7.85	ADP binding	6.38
response to organonitrogen compound	7.25	response to jasmonic acid	4.45
cellular response to hypoxia	5.81	defense response to bacterium	4.08
sulfur compound binding	5.81	innate immune response	3.79
jasmonic acid metabolic process	5.55	response to bacterium	3.53
calcium ion transmembrane transport	5.51	cellular response to stress	2.46
heat acclimation	4.83	response to abiotic stimulus	2.15
response to wounding	4.64	<i>Giardia</i> DOWNREGULATED	
defense response to bacterium, incompatible interaction	4.56	ion transport	3.14
negative regulation of cell death	4.51	intrinsic component of membrane	1.41
response to ozone	4.49	<i>Cryptosporidia</i> UPREGULATED	
secondary metabolite catabolic process	4.27	regulation of response to external stimulus	4.22
toxin catabolic process	4.27	dephosphorylation	3.52
response to high light intensity	4.13	organonitrogen compound catabolic process	3.39
response to oomycetes	4.00	heterocycle catabolic process	3.32
defense response to fungus, incompatible interaction	3.90	defense response, incompatible interaction	3.06
activation of innate immune response	3.69	regulation of response to stress	2.42
calcium ion transmembrane transporter activity	3.34	response to ethylene	2.37
quercetin 3-O-glucosyltransferase activity	3.13	protein transport	2.29
transmembrane receptor protein serine/threonine kinase activity	3.13	cellular macromolecule localization	2.20
plant-type hypersensitive response	3.11	intracellular transport	2.13
host programmed cell death induced by symbiont	3.08	chloroplast stroma	2.06
salicylic acid mediated signaling pathway	3.04	<i>Cryptosporidia</i> DOWNREGULATED	
ethylene-activated signaling pathway	2.69	specification of symmetry	19.48
COMMON DOWNREGULATED		glucosinolate biosynthetic process	7.97
positive regulation of development	15.79	response to cyclopentenone	6.88
syncytium formation	13.16	nucleosome	4.58
cell surface	10.53	phloem or xylem histogenesis	4.25
regulation of organ growth	9.97	glucosinolate metabolic process	4.25
plant-type cell wall modification involved in multidimensional cell growth	8.10	DNA packaging complex	4.18
response to insect	7.29	sulfur compound biosynthetic process	3.93
very long-chain fatty acid biosynthetic process	7.02	oligopeptide transport	3.90
hormone binding	7.02	meristem structural organization	3.84
CCAAT-binding factor complex	7.02	anatomical structure arrangement	3.64
3-oxo-lignoceryl-CoA synthase activity	7.02	enzyme linked receptor protein signaling pathway	3.60
wax biosynthetic process	7.02	transmembrane receptor protein tyrosine kinase signaling pathway	3.60
regulation of gibberellic acid mediated signaling pathway	6.65	response to salicylic acid	3.36
regulation of anion transport	6.65	shoot system morphogenesis	3.19
organ growth	6.53	cell surface receptor signaling pathway	3.00
asymmetric cell division	6.02	flavin adenine dinucleotide binding	2.98
auxin transport	5.26	response to organic cyclic compound	2.71
multidimensional cell growth	4.83	plant-type cell wall	2.32
positive gravitropism	4.75	chemical homeostasis	2.19
systemic acquired resistance	4.09	anchored component of membrane	2.17
leaf morphogenesis	3.92	apoplast	2.12
response to brassinosteroid	3.10		
shoot system morphogenesis	2.87		

3.2.1. Commonly Upregulated GO Terms

Among commonly upregulated GO terms, there were “cellular response to chitin”, “oligopeptide binding”, “response to organonitrogen compound”, “jasmonic acid metabolic process”, “response to wounding”, “defense response to bacterium, incompatible interaction”, “negative regulation of cell death”, “response to oomycetes”, “defense response to fungus”, “incompatible interaction”, and “activation of innate immune response” (Table 2).

Chitin is a structural component of cysts of fungi and various parasites, including *Giardia* and *Cryptosporidia* [28]. Plants are known to respond to chitin, primarily stemming from the fungal cell wall [29]. It is possible that response to chitin is uniform in plants, regardless of its origin.

Oligopeptide production is a part of normal activities of parasites, and plants and animals developed mechanisms for their recognition as a part of microbe-associated molecular patterns (MAMPs) defence mechanism [30].

GO term “response to organonitrogen compound” was enriched in cucumber plant exposed to parasitic dodder plant [31]. Infection of wheat and oat with larvae of wheat stem sawfly results in an increase in the level of organonitrogen compounds [32]. Such response appears to be common in animals. Serum of chickens infected with *Cryptosporidium baileyi* showed increased levels of organonitrogen compounds [33]. Exposure of human intestinal epithelial cells to *Giardia intestinalis* also resulted in enriched GO term “response to organonitrogen compound” [34].

Cellular response to hypoxia was also upregulated. The significance of this is not clear, but genes involved in hypoxic response in part overlap with the immune response in plants [35]. It is possible that the way we treated our plants with cysts (submerged in PBS) could contribute to the upregulation of hypoxia response genes.

“Sulfur compound binding” was also upregulated. Plants produce hydrogen sulfide (H₂S) in response to pathogen stress, and H₂S has been implemented in salicylic acid signalling and plant immune response [36]. Exogenous application of H₂S induces tolerance to temperature, water availability, and salt stresses [37].

Several GO terms associated with response to fungal pathogens were overrepresented, including “defense response to fungus, incompatible interaction”, “response to oomycetes”, and “quercetin 3-O-glucosyltransferase activity”. Quercetin is often produced in response to fungal infection of plants [38]. It is possible that cysts of *Giardia* and *Cryptosporidia* have similar effects on plants.

“Heat acclimation” was another GO term commonly enriched in response to pathogens. It appears that heat response and pathogen response induce similar sets of genes, including those encoding several heat shock proteins [39].

Among classical hormonal signalling pathways activated in response to various biotic stresses, “jasmonic acid metabolic process”, “salicylic acid mediated signaling pathway” and “ethylene-activated signaling pathway” were commonly upregulated. The ethylene pathway is commonly activated in response to insects [40] as well as in response to heat stress [41]. Salicylic acid and jasmonic acid pathways are activated in response to viral, bacterial, and fungal pathogens, especially during incompatible interactions [42]. Other two GO terms overrepresented in response to both parasites were “defense response to bacterium, incompatible interaction” and “defense response to fungi, incompatible interaction”, suggesting that exposure to these two pathogens in plants occurs through incompatible interactions, and that *Arabidopsis* has the mechanisms of recognition of these pathogens and prevention of infection.

3.2.2. Commonly Downregulated GO Terms

Among commonly downregulated GO terms, there were “positive regulation of development”, “syncytium formation”, “cell surface”, “regulation of organ growth”, “plant-type cell wall modification involved in multidimensional cell growth”, “response to insect”, “3-oxo-lignoceroyl-CoA synthase activity”, “wax biosynthetic process”, “organ growth”, “asymmetric cell division”, “auxin transport”, “multidimensional cell growth”, “systemic acquired resistance”, “leaf morphogenesis”, and “shoot system morphogenesis”.

Both pathogens downregulated the GO terms associated with cell and organ growth. This is a common response to infection with many pathogens in plants [43,44]. Downregulation of plant growth in part occurs through inhibition of hormonal signalling, as evident by downregulation of GO terms “hormone binding”, “response to brassinosteroid” and “regulation of gibberellic acid mediated signaling pathway”. The latter two are classical phytohormones promoting growth and development in plants [45,46].

Syncytium is the fusion of multiple cells, resulting in the multinucleate giant cell. Pathogen infection is known to cause the development of syncytium; for example, infection of roots with nematodes results in formation of feeding syncytium cells [47]. Syncytium formation also occurs in human cells infected with viruses [48]. No such mechanism was reported for *Giardia* or *Cryptosporidia* infection. It appears that both tested human parasites suppress this mechanism in *Arabidopsis*.

Downregulation of GO terms “3-oxo-lignoceroyl-CoA synthase activity”, “wax biosynthetic process” and “very long-chain fatty acid biosynthetic process” is likely a specific response triggered by these two human parasites, even though they are not *Arabidopsis* pathogens. Wax is an essential protector that often allows plants to withstand certain abiotic stresses as well as gives protection against pathogens [49]. Thus, *Giardia* and *Cryptosporidia* likely inhibit wax production in *Arabidopsis* to promote the chances of further infection [50].

3.2.3. GO Terms Uniquely Altered in *Giardia*

Among uniquely upregulated GO terms by *Giardia*, there were “response to heat”, “ADP binding”, “response to jasmonic acid”, “defense response to bacterium”, while among downregulated, there were “ion transport” and “intrinsic component of membrane”.

While “heat acclimation” was the common GO term, “heat response” was uniquely upregulated in *Giardia*, suggesting that this parasite triggers response in *Arabidopsis* that has more significant crosstalk with heat stress response as compared to *Cryptosporidia*. Activation of heat shock proteins in response to heat and infection is relatively common in plants [39] and animals [51].

“ADP binding” has a significance in regulation of redox reactions and energy metabolism [52], and in animals it may also be involved in immune response and platelet aggregation [53].

Activation of “response to jasmonic acid” GO term indicates that *Giardia* triggers a more significant pathogen response; jasmonic acid is activated by herbivory and bacterial pathogens [54]. Overrepresentation of the GO term “defense response to bacterium” in *Giardia* alone supports this notion.

Downregulation of “intrinsic component of membrane” and “ion transport” in *Giardia* alone likely suggests a more significant effect on the membrane structure, fluidity, and transport of ions as compared to *Cryptosporidia*. Activation of ion transport and changes in the membrane potential are common responses to many pathogens in plants [55]. For example, changes in Ca²⁺ in various cell compartments are perceived as second messengers, and increased cytoplasmic concentration of Ca²⁺ is perceived as one of the signals of pathogen recognition [56]. It is possible that *Giardia* has certain mechanisms of suppression

of this activity. Curiously, *Giardia* infection results in significant alterations in ion transport in human duodenum epithelium cells [57].

3.2.4. GO Terms Uniquely Altered in Cryptosporidia

In response to Cryptosporidia, upregulated GO terms were “regulation of response to external stimulus”, “organonitrogen compound catabolic process”, “heterocycle catabolic process”, “incompatible interaction”, “regulation of response to stress”, “response to ethylene”, and “intracellular transport”, while downregulated included “specification of symmetry”, “glucosinolate biosynthetic process”, “response to cyclopentenone”, “nucleosome”, “phloem or xylem histogenesis”, “DNA packaging complex”, “sulfur compound biosynthetic process”, “meristem structural organization”, “anatomical structure arrangement”, “response to salicylic acid”, “shoot system morphogenesis”, and “flavin adenine dinucleotide binding” (Table 2).

Upregulation of “organonitrogen compound catabolic process” in the Cryptosporidia group alone suggests that this parasite activates degradation of nitrogen-containing compounds. Plants require nitrogen for defence against pathogens [58], so it is possible that Cryptosporidia activate this process.

It is hard to understand why the “heterocycle catabolic process” GO term was upregulated. Pathogens release heterocyclic compounds upon infection, and thus it is possible that plants activate their degradation. On the other hand, heterocyclic compounds are anti-microbial [59], and thus, it is possible that plants produced and degraded them at a higher rate in response to Cryptosporidia but not to *Giardia*.

Upregulation of “incompatible interaction”, “regulation of response to stress”, “response to ethylene” GO terms suggest that Cryptosporidia trigger some incompatible interactions that are unique, although several incompatible interactions GO terms were upregulated commonly by both parasites.

Several GO terms associated with photosynthesis, growth, anatomical structures, and morphogenesis were downregulated uniquely in Cryptosporidia, including “specification of symmetry”, “phloem or xylem histogenesis”, “meristem structural organization”, “anatomical structure arrangement”, “shoot system morphogenesis”, and “flavin adenine dinucleotide binding”. This suggests that Cryptosporidia may interfere with proper plant development more than *Giardia*. While such an effect on plants is not known, in animals, infection with these pathogens causes retardation of development [60]. Classical plant pathogens, however, are known to inhibit plant growth and development [43,44,61].

In Brassicaceae (including *Arabidopsis*), glucosinolates are involved in plant protection and are activated by various abiotic stresses and in response to insects [62]. It is possible that downregulation of “glucosinolate biosynthetic process” is some sort of suppression of defences triggered by Cryptosporidia; it is also possible that it is a mechanism of prioritization of responses by exposed plants, where such a pathway may be considered unnecessary for protection against this parasite.

GO term “response to cyclopentenone” was uniquely downregulated in Cryptosporidia. Cyclopentenones are precursors of jasmonic acid and are activated in response to pathogen stress, especially herbivory [63]. In animals, cyclopentenones are biologically active lipid mediators involved in inflammation, cell proliferation, and angiogenesis [64]. It appears that Cryptosporidia has mechanisms to suppress this process.

Fairly unique GO terms that were downregulated in Cryptosporidia were “nucleosome” and “DNA packaging complex”. It is possible that this parasite releases a unique set of chemicals, such as adhesive proteins, glycoproteins, components of feeding organelles, digestive enzymes etc., that downregulate certain components of chromatin remodelling. The latter is an essential process in response to many pathogens, both in plants [65] and

animals [66]. We found only one article mentioning the potential effect of *Cryptosporidium* infection on epigenetic regulation of host cells—*C. parvum* infection of rats provoked an increase in premature hepatocyte polyploidization and hypertrophy, epigenetically reprogramming hepatocyte structure and function [67].

3.3. RT-PCR Confirmation of Selected Gene Sets

To further validate the sequencing data, we have chosen a set of overexpressed genes with $\log_2 > 8$, in common and *Giardia*- or *Cryptosporidia*-specific groups. RT-PCR analysis confirmed the expression of all tested genes, albeit not to the same degree as observed in sequencing (Table 1).

4. Conclusions

Our work showed that *Arabidopsis* has the machinery to respond to heat-killed human pathogens, *Giardia* and *Cryptosporidia*. The majority of responses overlapped, indicating that pathogenic components of these two parasites likely interact with similar receptors on the surface of *Arabidopsis* cells. In general, GO terms involved in pathogen recognition, plant defence and immunity, and phytohormone signalling were upregulated, while those involved in plant development, plant growth, and morphogenesis were downregulated. Among unique responses, *Giardia* caused downregulation in membrane structure and ion transport, while *Cryptosporidia* “heterocycle catabolic processes” were upregulated, while GO term “response to cyclopentenone” and GO terms associated with chromatin remodelling were downregulated.

Future work may include more in-depth analysis of various pathways as well as use of *Arabidopsis* mutants impaired in various types of pathogen recognition. One promising avenue to explore is the analysis of the potential of *Cryptosporidia* to cause epigenetic dysregulation in the host.

Supplementary Materials: The following supporting information can be downloaded at: <https://www.mdpi.com/article/10.3390/ijpb16010013/s1>, Supplementary Table S1. Read statistics. Supplementary Figure S1. Visualization of differentially expressed GO terms using AgriGO in the upregulated genes in *Cryptosporidia* common for DESeq and NOISeq. Refer to Figure S7 for color coding visualization. Supplementary Figure S2. Visualization of differentially expressed GO terms using AgriGO in the downregulated genes in *Cryptosporidia* common for DESeq and NOISeq. Refer to Figure S7 for color coding visualization. Supplementary Figure S3. Visualization of differentially expressed GO terms using AgriGO in the downregulated genes in *Cryptosporidia* unique for DESeq analysis. Refer to Figure S7 for color coding visualization. Supplementary Figure S4. Visualization of differentially expressed GO terms using AgriGO in the upregulated genes in *Giardia* common for DESeq and NOISeq. Refer to Figure S7 for color coding visualization. Supplementary Figure S5. Visualization of differentially expressed GO terms using AgriGO in the downregulated genes in *Giardia* common for DESeq and NOISeq. Refer to Figure S7 for color coding visualization. Supplementary Figure S6. Visualization of differentially expressed GO terms using AgriGO in the downregulated genes in *Giardia* unique for DESeq analysis. Refer to Figure S7 for color coding visualization. Supplementary Figure S7. Shows the color code legend for level of changes and regulation for GO terms visualized in Supplementary Figures S1–S6. Supplementary File S1. Description of file content in DESeq2 analysis of gene expression data for *Giardia*. Supplementary File S2. Description of file content in DESeq2 analysis of gene expression data for *Cryptosporidia*. Supplementary File S3. Description of file content in NOISeq analysis of gene expression data for *Giardia*. Supplementary File S4. Description of file content in NOISeq analysis of gene expression data for *Cryptosporidia*. Supplementary File S5. Full list of all unique and common GO terms identified by DESeq in *Giardia* and *Cryptosporidia*.

Author Contributions: Conceptualization, I.K. and A.G.; methodology, A.G., Y.I. and B.B.; validation, A.G., Y.I. and B.B.; formal analysis, A.G., Y.I. and B.B.; resources, I.K.; data curation, A.G., Y.I. and B.B.; writing—I.K., A.G., Y.I. and B.B.; supervision, I.K.; project administration, I.K.; funding acquisition, I.K. All authors have read and agreed to the published version of the manuscript.

Funding: We thank Natural Sciences and Engineering Research Council of Canada (NSERC), grant RGPIN 2016-06555 to I.K. for funding our work.

Institutional Review Board Statement: Not applicable.

Informed Consent Statement: Not applicable.

Data Availability Statement: Data are available upon request.

Acknowledgments: We would like to thank Hyperion Research Ltd. and Peter Wallis for producing heat-killed *Giardia* and *Cryptosporidia* for our research.

Conflicts of Interest: The authors declare no conflict of interest.

Abbreviations

The following abbreviations are used in this manuscript:

PRR	pattern recognition receptors
PAMPs	pathogen-associated molecular patterns
TLR	Toll-like receptors
LPS	lipopolysaccharides
NLRs	nucleotide-binding and oligomerization domain (NOD)-like receptors
PTI	pattern-triggered immunity
DAMPs	damage-associated molecular patterns
DEGs	Differentially expressed genes
MAMPs	microbe-associated molecular patterns

References

- Robertson, L.J. Parasites in Food: From a Neglected Position to an Emerging Issue. *Adv. Food Nutr. Res.* **2018**, *86*, 71–113. [[CrossRef](#)] [[PubMed](#)]
- Lim, J.-A.; Lee, D.H.; Heu, S. The interaction of human enteric pathogens with plants. *Plant Pathol. J.* **2014**, *30*, 109–116. [[CrossRef](#)] [[PubMed](#)]
- Serradell, M.C.; Rupil, L.L.; Martino, R.A.; Prucca, C.G.; Carranza, P.G.; Saura, A.; Fernández, E.A.; Gargantini, P.R.; Tenaglia, A.H.; Petiti, J.P.; et al. Efficient oral vaccination by bioengineering virus-like particles with protozoan surface proteins. *Nat. Commun.* **2019**, *10*, 361. [[CrossRef](#)] [[PubMed](#)]
- Li, D.; Wu, M. Pattern recognition receptors in health and diseases. *Signal Transduct. Target. Ther.* **2021**, *6*, 291. [[CrossRef](#)]
- Amarante-Mendes, G.P.; Adjemian, S.; Branco, L.M.; Zanetti, L.C.; Weinlich, R.; Bortoluci, K.R. Pattern Recognition Receptors and the Host Cell Death Molecular Machinery. *Front. Immunol.* **2018**, *9*, 2379. [[CrossRef](#)]
- Jo, E.-K. Interplay between host and pathogen: Immune defense and beyond. *Exp. Mol. Med.* **2019**, *51*, 1–3. [[CrossRef](#)]
- Klimczak, S.; Packi, K.; Rudek, A.; Wenclewska, S.; Kurowski, M.; Kurczabińska, D.; Śliwińska, A. The Influence of the Protozoan *Giardia lamblia* on the Modulation of the Immune System and Alterations in Host Glucose and Lipid Metabolism. *Int. J. Mol. Sci.* **2024**, *25*, 8627. [[CrossRef](#)] [[PubMed](#)]
- Espinosa-Riquer, Z.P.; Segura-Villalobos, D.; Ramírez-Moreno, I.G.; Pérez Rodríguez, M.J.; Lamas, M.; Gonzalez-Espinosa, C. Signal Transduction Pathways Activated by Innate Immunity in Mast Cells: Translating Sensing of Changes into Specific Responses. *Cells* **2020**, *9*, 2411. [[CrossRef](#)] [[PubMed](#)]
- Shirron, N.; Yaron, S. Active suppression of early immune response in tobacco by the human pathogen *Salmonella Typhimurium*. *PLoS ONE* **2011**, *6*, e18855. [[CrossRef](#)]
- Garcia, A.V.; Charrier, A.; Schikora, A.; Bigeard, J.; Pateyron, S.; de Tauzia-Moreau, M.-L.; Evrard, A.; Mithöfer, A.; Martin-Magniette, M.L.; Virlogeux-Payant, I.; et al. *Salmonella enterica* flagellin is recognized via FLS2 and activates PAMP-triggered immunity in *Arabidopsis thaliana*. *Mol. Plant* **2014**, *7*, 657–674. [[CrossRef](#)]
- Segonzac, C.; Zipfel, C. Activation of plant pattern-recognition receptors by bacteria. *Curr. Opin. Microbiol.* **2011**, *14*, 54–61. [[CrossRef](#)] [[PubMed](#)]

12. Hegenauer, V.; Fürst, U.; Kaiser, B.; Smoker, M.; Zipfel, C.; Felix, G.; Stahl, M.; Albert, M. Detection of the plant parasite *Cuscuta reflexa* by a tomato cell surface receptor. *Science* **2016**, *353*, 478–481. [[CrossRef](#)]
13. Wang, Y.; Dang, F.; Liu, Z.; Wang, X.; Eulgem, T.; Lai, Y.; Yu, L.; She, J.; Shi, Y.; Lin, J.; et al. CaWRKY 58, encoding a group I WRKY transcription factor of *Capsicum annuum*, negatively regulates resistance to *Ralstonia solanacearum* infection. *Mol. Plant Pathol.* **2012**, *14*, 131–144. [[CrossRef](#)] [[PubMed](#)]
14. Golubov, A.; Byeon, B.; Woycicki, R.; Laing, C.; Gannon, V.; Kovalchuk, I. Transcriptomic profiling of *Arabidopsis thaliana* plants exposed to the human pathogen *Escherichia coli* O157-H7. *Biocatal. Agric. Biotechnol.* **2016**, *8*, 86–96. [[CrossRef](#)]
15. Golubov, A.; Byeon, B.; Woycicki, R.; Inglis, G.D.; Kovalchuk, I. Transcriptome of *Arabidopsis thaliana* plants treated with the human pathogen *Campylobacter jejuni*. *Biocatal. Agric. Biotechnol.* **2017**, *11*, 259–267. [[CrossRef](#)]
16. Martínez-Ocaña, J.; Maravilla, P.; Olivo-Díaz, A. Interaction between human mucins and parasite glycoproteins: The role of lectins and glycosidases in colonization by intestinal protozoa. *Rev. Inst. Med. Trop. Sao Paulo* **2020**, *62*, e64. [[CrossRef](#)] [[PubMed](#)]
17. Sateriale, A.; Gullicksrud, J.A.; Engiles, J.B.; McLeod, B.L.; Kugler, E.M.; Henao-Mejia, J.; Zhou, T.; Ring, A.M.; Brodsky, I.E.; Hunter, C.A.; et al. The intestinal parasite *Cryptosporidium* is controlled by an enterocyte intrinsic inflammasome that depends on NLRP6. *Proc. Natl. Acad. Sci. USA* **2020**, *118*, e2007807118. [[CrossRef](#)] [[PubMed](#)]
18. Trapnell, C.; Pachter, L.; Salzberg, S.L. TopHat: Discovering splice junctions with RNA-Seq. *Bioinformatics* **2009**, *25*, 1105–1111. [[CrossRef](#)] [[PubMed](#)]
19. Trapnell, C.; Williams, B.A.; Pertea, G.; Mortazavi, A.; Kwan, G.; Van Baren, M.J.; Salzberg, S.L.; Wold, B.J.; Pachter, L. Transcript assembly and quantification by RNA-Seq reveals unannotated transcripts and isoform switching during cell differentiation. *Nat. Biotechnol.* **2010**, *28*, 511–515. [[CrossRef](#)] [[PubMed](#)]
20. Trapnell, C.; Roberts, A.; Goff, L.; Pertea, G.; Kim, D.; Kelley, D.R.; Pimentel, H.; Salzberg, S.L.; Rinn, J.L.; Pachter, L. Differential gene and transcript expression analysis of RNA-seq experiments with TopHat and Cufflinks. *Nat. Protoc.* **2012**, *7*, 562–578. [[CrossRef](#)]
21. Durbin, B.; Hardin, J.; Hawkins, D.; Rocke, D. A variance-stabilizing transformation for gene-expression microarray data. *Bioinformatics* **2002**, *18* (Suppl. S1), S105–S110. [[CrossRef](#)] [[PubMed](#)]
22. Robinson, M.D.; Oshlack, A. A scaling normalization method for differential expression analysis of RNA-seq data. *Genome Biol.* **2010**, *11*, R25. [[CrossRef](#)] [[PubMed](#)]
23. Falcon, S.; Gentleman, R. Using GOstats to test gene lists for GO term association. *Bioinformatics* **2006**, *23*, 257–258. [[CrossRef](#)]
24. Luo, W.; Brouwer, C. Pathview: An R/Bioconductor package for pathway-based data integration and visualization. *Bioinformatics* **2013**, *29*, 1830–1831. [[CrossRef](#)] [[PubMed](#)]
25. Sun, L.; Li, J.; Xie, F.; Wu, S.; Shao, T.; Li, X.; Li, J.; Jian, F.; Zhang, S.; Ning, C.; et al. Whole transcriptome analysis of HCT-8 cells infected by *Cryptosporidium parvum*. *Parasites Vectors* **2022**, *15*, 441. [[CrossRef](#)]
26. Tako, E.A.; Hassimi, M.F.; Li, E.; Singer, S.M. Transcriptomic analysis of the host response to *Giardia duodenalis* infection reveals redundant mechanisms for parasite control. *MBio* **2013**, *4*, 10–1128. [[CrossRef](#)] [[PubMed](#)]
27. Yang, D.; Liu, Y.; Ren, Y.; Hao, L.; Zhang, X.; Chen, H.; Liu, J. *Giardia intestinalis* extracellular vesicles induce changes in gene expression in human intestinal epithelial cells in vitro. *Exp. Parasitol.* **2024**, *262*, 108788. [[CrossRef](#)] [[PubMed](#)]
28. Samuelson, J.; Bushkin, G.G.; Chatterjee, A.; Robbins, P.W. Strategies to discover the structural components of cyst and oocyst walls. *Eukaryot. Cell* **2013**, *12*, 1578–1587. [[CrossRef](#)] [[PubMed](#)]
29. Pusztahelyi, T. Chitin and chitin-related compounds in plant-fungal interactions. *Mycology* **2018**, *9*, 189–201. [[CrossRef](#)]
30. Albert, M. Peptides as triggers of plant defence. *J. Exp. Bot.* **2013**, *64*, 5269–5279. [[CrossRef](#)] [[PubMed](#)]
31. Zhang, J.; Xu, Y.; Xie, J.; Zhuang, H.; Liu, H.; Shen, G.; Wu, J. Parasite dodder enables transfer of bidirectional systemic nitrogen signals between host plants. *Plant Physiol.* **2020**, *185*, 1395–1410. [[CrossRef](#)] [[PubMed](#)]
32. Hager, M.S.; Hofland, M.L.; Varella, A.C.; Bothner, B.; Budak, H.; Weaver, D.K. Untargeted metabolomics profiling of oat (*Avena sativa* L.) and wheat (*Triticum aestivum* L.) infested with wheat stem sawfly (*Cephus cinctus* Norton) reveals differences associated with plant defense and insect nutrition. *Front. Plant Sci.* **2024**, *15*, 1327390. [[CrossRef](#)]
33. Wu, X.-M.; Yang, X.; Fan, X.-C.; Chen, X.; Wang, Y.-X.; Zhang, L.-X.; Song, J.-K.; Zhao, G.-H. Serum metabolomics in chickens infected with *Cryptosporidium baileyi*. *Parasites Vectors* **2021**, *14*, 336. [[CrossRef](#)]
34. Peirasmaki, D.; Ma'ayeh, S.Y.; Xu, F.; Ferella, M.; Campos, S.; Liu, J.; Svärd, S.G. High Cysteine Membrane Proteins (HCMPs) Are Upregulated During *Giardia*-Host Cell Interactions. *Front. Genet.* **2020**, *11*, 913. [[CrossRef](#)] [[PubMed](#)]
35. Basit, F.; Khalid, M.; El-Keblawy, A.; Sheteiwy, M.S.; Sulieman, S.; Josko, I.; Zulfikar, F. Hypoxia stress: Plant's sensing, responses, and tolerance mechanisms. *Environ. Sci. Pollut. Res.* **2024**, *31*, 63458–63472. [[CrossRef](#)]
36. Vojtovič, D.; Luhová, L.; Petřivalský, M. Something smells bad to plant pathogens: Production of hydrogen sulfide in plants and its role in plant defence responses. *J. Adv. Res.* **2020**, *27*, 199–209. [[CrossRef](#)] [[PubMed](#)]
37. Li, Z.-G.; Min, X.; Zhou, Z.-H. Hydrogen Sulfide: A Signal Molecule in Plant Cross-Adaptation. *Front. Plant Sci.* **2016**, *7*, 1621. [[CrossRef](#)] [[PubMed](#)]

38. Ren, J.; Tang, W.; Barton, C.D.; Price, O.M.; Mortensen, M.W.; Phillips, A.; Wald, B.; Hulme, S.E.; Stanley, L.P.; Hevel, J.; et al. A highly versatile fungal glucosyltransferase for specific production of quercetin-7-O-beta-D-glucoside and quercetin-3-O-beta-D-glucoside in different hosts. *Appl. Microbiol. Biotechnol.* **2021**, *106*, 227–245. [[CrossRef](#)] [[PubMed](#)]
39. Lee, J.-H.; Yun, H.S.; Kwon, C. Molecular communications between plant heat shock responses and disease resistance. *Mol. Cells* **2012**, *34*, 109–116. [[CrossRef](#)]
40. Verma, V.; Ravindran, P.; Kumar, P.P. Plant hormone-mediated regulation of stress responses. *BMC Plant Biol.* **2016**, *16*, 86. [[CrossRef](#)] [[PubMed](#)]
41. Huang, J.; Zhao, X.; Bürger, M.; Chory, J.; Wang, X. The role of ethylene in plant temperature stress response. *Trends Plant Sci.* **2023**, *28*, 808–824. [[CrossRef](#)] [[PubMed](#)]
42. Hou, S.; Tsuda, K. Salicylic acid and jasmonic acid crosstalk in plant immunity. *Essays Biochem.* **2022**, *66*, 647–656. [[CrossRef](#)] [[PubMed](#)]
43. Jiang, C.-J.; Liu, X.-L.; Liu, X.-Q.; Zhang, H.; Yu, Y.-J.; Liang, Z.-W. Stunted Growth Caused by Blast Disease in Rice Seedlings Is Associated with Changes in Phytohormone Signaling Pathways. *Front. Plant Sci.* **2017**, *8*, 1558. [[CrossRef](#)]
44. Reitz, M.U.; Gifford, M.L.; Schäfer, P. Hormone activities and the cell cycle machinery in immunity-triggered growth inhibition. *J. Exp. Bot.* **2015**, *66*, 2187–2197. [[CrossRef](#)] [[PubMed](#)]
45. Nolan, T.M.; Vukašinić, N.; Liu, D.; Russinova, E.; Yin, Y. Brassinosteroids: Multidimensional Regulators of Plant Growth, Development, and Stress Responses. *Plant Cell* **2019**, *32*, 295–318. [[CrossRef](#)] [[PubMed](#)]
46. Hedden, P. The Current Status of Research on Gibberellin Biosynthesis. *Plant Cell Physiol.* **2020**, *61*, 1832–1849. [[CrossRef](#)]
47. Matuszkiewicz, M.; Sobczak, M.; Cabrera, J.; Escobar, C.; Karpiński, S.; Filipecki, M. The Role of Programmed Cell Death Regulator LSD1 in Nematode-Induced Syncytium Formation. *Front. Plant Sci.* **2018**, *9*, 314. [[CrossRef](#)]
48. Andrade, A.d.S.; Campos, S.O.; Dias, J.; Campos, M.A.; Kroon, E.G. Dengue virus 3 genotype I (GI) lineage 1 (L1) isolates elicit differential cytopathic effect with syncytium formation in human glioblastoma cells (U251). *Virology* **2023**, *20*, 204. [[CrossRef](#)]
49. Kunst, L.; Samuels, A.L. Biosynthesis and secretion of plant cuticular wax. *Prog. Lipid Res.* **2003**, *42*, 51–80. [[CrossRef](#)] [[PubMed](#)]
50. Lewandowska, M.; Keyl, A.; Feussner, I. Wax biosynthesis in response to danger: Its regulation upon abiotic and biotic stress. *New Phytol.* **2020**, *227*, 698–713. [[CrossRef](#)] [[PubMed](#)]
51. Stewart, G.R.; Young, D.B. Heat-shock proteins and the host-pathogen interaction during bacterial infection. *Curr. Opin. Immunol.* **2004**, *16*, 506–510. [[CrossRef](#)]
52. Huang, L.; Wang, J.; Lilley, D.M. Structure and ligand binding of the ADP-binding domain of the NAD(+) riboswitch. *RNA* **2020**, *26*, 878–887. [[CrossRef](#)] [[PubMed](#)]
53. Entsie, P.; Kang, Y.; Amofo, E.B.; Schöneberg, T.; Liverani, E. The Signaling Pathway of the ADP Receptor P2Y(12) in the Immune System: Recent Discoveries and New Challenges. *Int. J. Mol. Sci.* **2023**, *24*, 6709. [[CrossRef](#)] [[PubMed](#)]
54. Carvalhais, L.C.; Dennis, P.G.; Badri, D.V.; Tyson, G.W.; Vivanco, J.M.; Schenk, P.M. Activation of the jasmonic acid plant defence pathway alters the composition of rhizosphere bacterial communities. *PLoS ONE* **2013**, *8*, e56457. [[CrossRef](#)] [[PubMed](#)]
55. Simmi, F.; Dallagnol, L.; Ferreira, A.; Pereira, D.; Souza, G. Electrometric alterations in a plant-pathogen system: Toward early diagnosis. *Bioelectrochemistry* **2020**, *133*, 107493. [[CrossRef](#)] [[PubMed](#)]
56. Koster, P.; De Falco, T.A.; Zipfel, C. Ca²⁺ signals in plant immunity. *EMBO J.* **2022**, *41*, e110741. [[CrossRef](#)] [[PubMed](#)]
57. Troeger, H.; Epple, H.J.; Schneider, T.; Wahnschaffe, U.; Ullrich, R.; Burchard, G.D.; Jelinek, T.; Zeitz, M.; Fromm, M.; Schulzke, J.D. Effect of chronic *Giardia lamblia* infection on epithelial transport and barrier function in human duodenum. *Gut* **2007**, *56*, 328–335. [[CrossRef](#)]
58. Mur, L.A.J.; Simpson, C.; Kumari, A.; Gupta, A.K.; Gupta, K.J. Moving nitrogen to the centre of plant defence against pathogens. *Ann. Bot.* **2017**, *119*, 703–709. [[CrossRef](#)] [[PubMed](#)]
59. Darwish, E.S. Facile synthesis and antimicrobial evaluation of some new heterocyclic compounds incorporating a biologically active sulfamoyl moiety. *Sci. World J.* **2014**, *2014*, 165495. [[CrossRef](#)] [[PubMed](#)]
60. Ramirez, N.E.; Ward, L.A.; Sreevatsan, S. A review of the biology and epidemiology of cryptosporidiosis in humans and animals. *Microbes Infect.* **2004**, *6*, 773–785. [[CrossRef](#)] [[PubMed](#)]
61. Kong, F.; Yang, L. Pathogen-triggered changes in plant development: Virulence strategies or host defense mechanism? *Front. Microbiol.* **2023**, *14*, 1122947. [[CrossRef](#)] [[PubMed](#)]
62. Nguyen, V.P.T.; Stewart, J.; Lopez, M.; Ioannou, I.; Allais, F. Glucosinolates: Natural Occurrence, Biosynthesis, Accessibility, Isolation, Structures, and Biological Activities. *Molecules* **2020**, *25*, 4537. [[CrossRef](#)] [[PubMed](#)]
63. Howe, G.A. Cyclopentenone signals for plant defense: Remodeling the jasmonic acid response. *Proc. Natl. Acad. Sci. USA* **2001**, *98*, 12317–12319. [[CrossRef](#)] [[PubMed](#)]
64. Lee, B.R.; Paing, M.H.; Sharma-Walia, N. Cyclopentenone Prostaglandins: Biologically Active Lipid Mediators Targeting Inflammation. *Front. Physiol.* **2021**, *12*, 640374. [[CrossRef](#)]
65. Berr, A.; Ménard, R.; Heitz, T.; Shen, W.-H. Chromatin modification and remodelling: A regulatory landscape for the control of Arabidopsis defence responses upon pathogen attack. *Cell. Microbiol.* **2012**, *14*, 829–839. [[CrossRef](#)] [[PubMed](#)]

66. Liao, J.; Ho, J.; Burns, M.; Dykhuizen, E.C.; Hargreaves, D.C. Collaboration between distinct SWI/SNF chromatin remodeling complexes directs enhancer selection and activation of macrophage inflammatory genes. *Immunity* **2024**, *57*, 1780–1795.e6. [[CrossRef](#)] [[PubMed](#)]
67. Anatskaya, O.V.; Sidorenko, N.V.; Vinogradov, A.E.; Beyer, T.V. Impact of neonatal cryptosporidial gastroenteritis on epigenetic programming of rat hepatocytes. *Cell Biol. Int.* **2007**, *31*, 420–427. [[CrossRef](#)]

Disclaimer/Publisher’s Note: The statements, opinions and data contained in all publications are solely those of the individual author(s) and contributor(s) and not of MDPI and/or the editor(s). MDPI and/or the editor(s) disclaim responsibility for any injury to people or property resulting from any ideas, methods, instructions or products referred to in the content.